Applied Geochemistry 204 (2026) 106859

Contents lists available at ScienceDirect

Applied Geochemistry

journal homepage: www.elsevier.com/locate/apgeochem

Geochemical, mineralogical and particle-size controls on origin, transport and storage of sediment-associated metal(loid)s in an acid mine drainage-affected river

Elin Jennings [a,b,f,*], Patrizia Onnis [c], Rich Crane [a,b], William M. Mayes [d], Adam P. Jarvis [e], Karen A. Hudson-Edwards [a,b]

[a] Camborne School of Mines, Department of Earth and Environmental Sciences, University of Exeter, Penryn, TR10 9FE, UK
[b] Environment and Sustainability Institute, University of Exeter, Penryn, TR10 9FE, UK
[c] Department of Chemical and Geological Sciences, University of Cagliari, Monserrato, 09042, Italy
[d] School of Environmental Sciences, University of Hull, Hull, HU6 7RX, UK
[e] School of Engineering, Newcastle University, Newcastle upon Tyne, NE1 7RU, UK
[f] Now at W.H. Bryan Mining & Geology Research Centre, Sustainable Minerals Institute, The University of Queensland, Brisbane, Australia

ARTICLE INFO

Editorial handling by: Elisa Sacchi

Keywords:
Acid mine drainage
Sediment contamination
Legacy mine waste
Fe oxides
Arsenic
Particle size distribution

ABSTRACT

Acid mine drainage (AMD) continues to contaminate river systems worldwide, yet the interactions of metal(loid)s with sediments and the controls on their storage and remobilisation remain poorly constrained. This study examines the geochemical and mineralogical factors governing sediment-associated As, Cu, and Zn along an AMD-impacted river system (Carnon River, UK). To assess the interaction of metal(loid)s in sediments, their mineral hosts, and distribution over different particle sizes were investigated. Sediment concentrations reached 8210 mg/kg As, 5040 mg/kg Cu, 2760 mg/kg Zn, and 137,000 mg/kg Fe, substantially above guideline values and persisting downstream of the initial AMD input. Sulfide and sulfate minerals hosted Zn and Fe oxides were the primary hosts for As and Cu. Arsenic was strongly correlated with Fe, suggesting association with secondary Fe-oxide. Elevated downstream concentrations of such ecotoxic metal(loid)s within sediments indicated continuous input from both AMD precipitation and remobilised historic waste and limited natural attenuation. This integrated approach reveals a bimodal distribution: sorption/co-precipitation with secondary Fe-oxide or coarse sulfide sources that sustained contamination decades after mining ceased. These findings demonstrate how sediment mineralogy and particle size dictate contaminant mobility and long-term storage in AMD-affected catchments.

1. Introduction

Acid mine drainage (AMD) is a global issue affecting an estimated 20,000–50,000 mines worldwide that discharge into surrounding river systems (Rezaie and Anderson, 2020; Macklin et al., 2023). It is caused by the oxidation of sulfide minerals (primarily pyrite) (Akcil and Koldas, 2006; Simate and Ndlovu, 2014; Crane and Sapsford, 2018) and typically exhibits low pH and high concentrations of SO_4^{2-}, Fe, SiO_2, Al and metal(loid)s (including As, Cu, and Zn) (Environment Agency, 2008; Nordstrom et al., 2015). AMD treatment is often complex and expensive (Johnson and Hallberg, 2005; Akcil and Koldas, 2006; Wolkersdorfer, 2008), with estimates for total global AMD remediation costs often in the order of US$ $100bn (Hudson-Edwards et al., 2011; Lottermoser, 2015; Tremblay and Hogan, 2016). As a result, AMD-affected rivers are often left untreated, which presents a complex and widespread environmental issue.

AMD can cause the release of metal(loid)s into river waters, and these elements can also precipitate to form particles, some of which behave as colloids and remain highly mobile, or sorb onto streambed sediments, (i.e. Cánovas et al., 2012; Papaslioti et al., 2024). While substantial research has been conducted on aqueous phase contamination from AMD (e.g. Hierro et al., 2014; Moreno-González et al., 2022; Jennings et al., 2025), there has been few studies which have investigated the environmental behaviour and fate of particulates in these environments (Byrne et al., 2013; Onnis et al., 2023a).

In AMD-affected river systems, particulate contamination differs

* Corresponding author. Camborne School of Mines, Department of Earth and Environmental Sciences, University of Exeter, Penryn, TR10 9FE, UK.
E-mail address: elin.jennings@uq.edu.au (E. Jennings).

https://doi.org/10.1016/j.apgeochem.2026.106859
Received 16 February 2026; Received in revised form 19 April 2026; Accepted 28 April 2026
Available online 28 April 2026

from other mining affected rivers due to the formation of Fe oxides and oxyhydroxides that readily co-precipitate with or sorb metal(loid)s when the AMD mixes with higher pH receiving waters (e.g. Odiel River (Spain) (Navarro Torres et al., 2012), Gold King Mine Colorado Animas River accident 2015 (USA) (Rodriguez-Freire et al., 2016) and Rio Tinto (Spain) (Cánovas et al., 2014)). The composition of these secondary minerals is determined by a wide range of factors, including aqueous metal(loid) concentration, pH and redox. As a result, metal (loid)-bearing precipitates can act as sinks, decreasing aqueous metal (loid) concentrations via co-precipitation or sorption. Their fine particle size, however, makes them susceptible to remobilisation under changing environmental conditions. (Macklin et al. (1997), Hudson-Edwards et al. (1999), and Sánchez España et al. (2006) identified Fe oxyhydroxysulfates and Fe (oxy)hydroxides as the main storage of contaminants in mining-affected river sediments. These secondary minerals may also contribute to metal(loid) mobilisation through leaching, erosion, or desorption, thereby influencing transport and availability within river systems (Dold, 2014; Ortiz-Castillo et al., 2021). However, the understanding of how significant these Fe oxides are to the sediment load of AMD-affected rivers, and on the role of particle size and mineralogy in governing long-term contaminant source, transport and deposition in these rivers, is limited. Given that AMD formation is invariably a long-term or even quasi-permanent process (e.g. Coulthard and Macklin, 2003), knowledge of these fundamental processes governing transport and fate is crucial for their sustainable and effective management.

The impacts of AMD on river systems are inherently spatially and temporally complex, governed by various factors such as river flow regime (Turner et al., 2008; Onnis et al., 2023b; Jennings et al., 2025), geomorphology (Macklin et al., 2006; Onnis et al., 2023a) and geochemical conditions (pH, redox, ionic strength) (Casiot et al., 2005; Butler, 2009; Cánovas et al., 2018). These factors influence the mobilisation, transport, and deposition of contaminated sediments, which can be remobilised during high flow events and deposited in floodplains (Foulds et al., 2012). Fluctuations in pH (Equeenuddin et al., 2013), redox (Lynch et al., 2014), and ionic strength (Millward, 1995; Braungardt et al., 2003; Lynch et al., 2014) as well as physical changes, such as erosion and tidal inundation (Millward, 1995; Pirrie et al., 2003; Izaditame et al., 2022) also play a key role in metal(loid) mobilisation. In addition, periodic flood events contribute to the metal(loid) mobilisation, such as increasing surface runoff, erosion of contaminated river embankments (and subsequent deposition during lower flows) and changes in redox conditions, leading to reductive dissolution of Fe oxides and their subsequent release of sorbed metal(loid)s (Byrne et al., 2013).

Whilst several studies have investigated metal(loid) distribution over different particle sizes of AMD-affected sediments (Song et al., 1999; Kim et al., 2011; Gerdelidani et al., 2021), there is limited information on the spatial variation of metal(loid)s across the sediment continuum, from source to estuary, in AMD-affected rivers and their associated mineralogical phases. Particularly, more research is needed on the mechanisms driving the remobilisation and redistribution of metal(loid)s along river systems and to assess how variations in geochemical conditions (e.g., pH, redox potential, and ionic strength) affect metal(loid) stability and mobility.

This study aimed to address this gap by providing mechanistic insights into the behaviour of metal(loid)s in an AMD-affected river system from source to estuary. Sediment samples were collected along the river, from source to estuary, to examine the spatial distribution of contaminant metal(loid)s in relation to particle size and mineralogy. The primary objective was to understand the role of river sediments in AMD-impacted systems, specifically their function as either a source or a sink for metal(loid)s. The results of this work will contribute to the development of more effective river management policies and inform future strategies for mitigating the environmental risks posed by AMD-affected rivers.

2. Methods and materials

2.1. Area of study

The Carnon River is located in Cornwall, United Kingdom (Fig. 1). It is 14 km long, has a catchment area of 31 km^2, and discharges into the tidally affected Restronguet Creek (50.2000 N, −5.065 W) (Environment Agency, 2020a, 2020b) (Fig. 1). The Carnon River is underlain by silt and sandstones from the Mylor Slate Formation, hosting enriched mineral veins containing As–Cu–Fe–Pb–Zn sulfides, cassiterite (SnO_2) and wolframite ($(Fe,Mn)WO_4$) (Embrey and Symes, 1987; Scrivener and Shepherd, 1998; Pirrie et al., 2002). The enriched mineral veins in the Carnon River catchment have made it a focus for mining activity for thousands of years (Buckley, 1992). Mining in the Carnon River catchment has been documented as spanning from the Bronze Age until the closure of Wheal* Jane in 1991 (Buckley, 1992; Pirrie et al., 2003; Neal et al., 2005; Rainbow, 2020) (*to note 'wheal' is a anglicised word for a mine or mine workings). Metal(loid)s of particular interest for mining in the Carnon River catchment include Cu and As, which were heavily sought after in the 18th and 19th centuries, expanding the mining enterprise in the area (Buckley, 1992).

Consequently, AMD has likely impacted the Carnon River for several (Buckley, 1992). The Carnon River is subject to the input of AMD via discharge from legacy mine adits (such as the County Adit, Nangiles Adit, and Wellington Adit) and from surface runoff from tailings, leachate, erosion of mine waste (ore material and tailings). These anthropogenic contributions enhance the output from natural processes, such as erosion of river embankments and groundwater input (Hunt and Howard, 1994; Pirrie et al., 2002, 2003; Jennings et al., 2025).

Amongst the most prominent AMD contributors to the Carnon River is the County Adit, which drains over 60 km of historical mine workings and is a significant source of metal(loid)s (Mayes et al., 2010). The County Adit, in its operational peak (the 1890s), discharged over 65 million litres a day of metal(loid) contaminated water directly into the Carnon River (Johnson and Thornton, 1987; Mayes et al., 2010; Rainbow, 2020). Currently, the County Adit discharges ~22 million litres a day of metal(loid) loaded water into the Carnon River (Jennings et al., 2025). This long history of discharging metal(loid) loaded waters has led to the deposition of contaminants down the length of the Carnon River, particularly in the estuary (known as 'Restronguet Creek'). Average river (Bryan and Gibbs, 1983) and estuarine (Pirrie et al., 2003) sediment concentrations have been reported as 1732 and 2800 mg/kg As, 2148 and 5070 mg/kg Cu, 297 and 570 mg/kg Pb, 2700 and 6600 mg/kg Zn, respectively. The Carnon River has also been affected by infrequent large-scale sudden AMD deposition events, such as the flooding of the Wheal Jane Mine in January 1992 when approximately 50 million litres of acidic (pH 3.1) metal(loid)-bearing AMD was discharged (Banks et al., 1997; Pirrie et al., 2002).

Many studies of the Carnon River (i.e. Banks et al., 1997; Pirrie et al., 2002; Jennings et al., 2025) have demonstrated that, although aqueous contamination is important for contaminant transport, their transport within solid phase particulates also plays a significant role. In particular, Jennings et al. (2025) showed that metal(loid)-bearing Fe oxide ochres that formed at the confluence of the County Adit and the Carnon River were significant in transporting and storing metal(loid)s with maximum total monthly loads into the estuary recorded at 354 (As), 742 (Cu), 1960 (Fe), 3320 (Zn) kg/month. Jennings et al. (2025) proposed that these Fe oxides were significant sources of sediments and metal(loid)s to the Carnon River through physical and chemical weathering.

2.2. Sample collection and preparation

Sixteen sample site locations were selected, where possible due to access issues, mostly at equal intervals down the entire length of the river and one site in the estuary. Additionally, samples were taken upstream and downstream of the confluences of major tributaries within

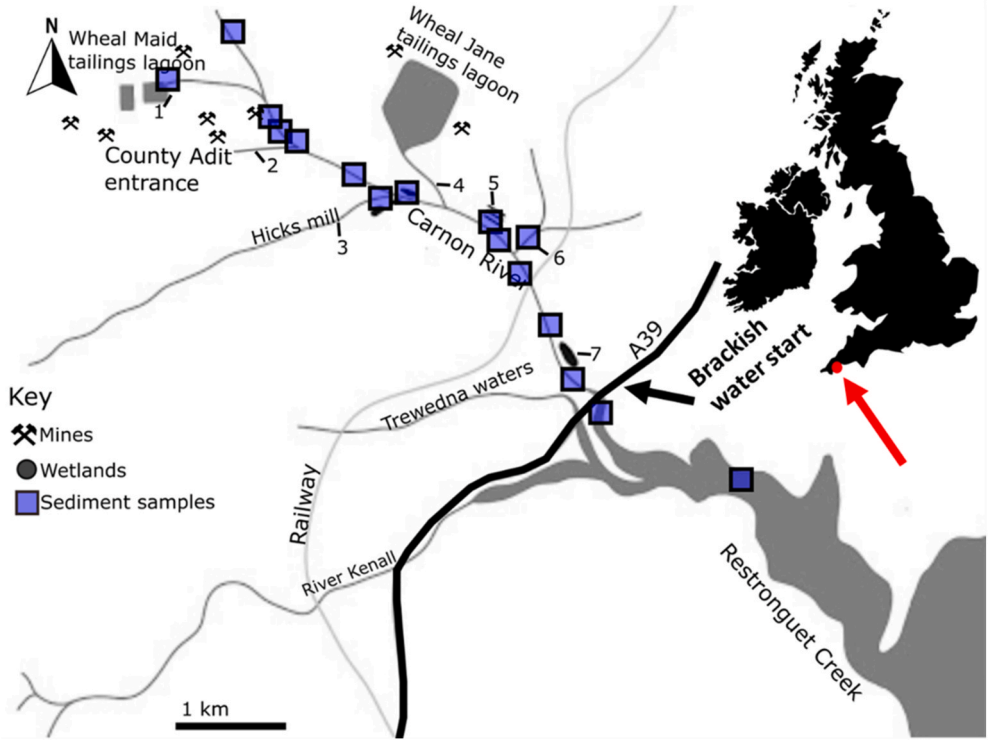

Fig. 1. Location of the Carnon River and sample sites. Numbered sites refer to Adit input and Carnon River tributaries. Input 1 is Wheal Maid (0.4 km). Input 2 is the County Adit (bank sediment) (Wellington and Nangiles Adit nearby) (0.88 km). Input 3 is Hicks mill tributary (not sampled) (1.81 km). Input 4 is Wheal Jane tributary (not sampled) (2.17 km). Input 5 is the potential Adit (2.77 km). Input 6 is the Grenna Lane bridge tributary (3.12 km). Input 7 is a wetland at Devoran Bridge (not sampled) (4.46 km). Sample details are in S1 in the supplementary information (S.I.). Downstream of the A39 road is the fresh- and seawater mixing zone (brackish water) (4.6 km).

the Carnon River catchment (Fig. 1, see S1 in SI for sample details). A triplicate sample was taken at one site during the sampling campaign for quality assurance. Twenty channel sediment samples were collected from the river embankment using a stainless-steel trowel and stored in air-tight bags. Sediment samples (~500 g) were collected at the surface (~5 cm) along a 2 m stretch and homogenised at each site to ensure a good representation of the riverine sediment. Sediments were oven-dried at 30 °C. Samples were riffled for non-bias separation into mineralogical and physical characteristic analysis and later used for geochemical analysis. All samples had particle size distribution (PSD) analysis due to their positioning in the Carnon River and proximity to sources. PSD was completed using the BS ISO 11277:2020 method (BSI, 2020) using Endcotts sieves on a vibration platform (Pascal sieve shaker), using sieve sizes; <0.063, 0.063-0.125, 0.125-0.25, 0.25-0.5, 0.5-1, 1-2, >2 mm. A tungsten carbide mill was used to pulverise the samples to <63 μm for geochemical analysis. For quality assurance, a blank of SiO_2 was pulverised (1 per 20 sediment samples) for geochemical analysis to ensure what level of contamination occurred during pulverising.

Field measurements of pH (HACH sensION + mm156 multiprobe) and GPS (GARMIN etrex 10) were taken in the waters next to the respective sediment sampling locations. The pH was calibrated each using appropriate calibration solutions (Hanna Instruments; pH 4.01, 7.01, and 10.01), prior to the sampling campaign.

2.3. Geochemical analysis

Total acid digestion was conducted using the four-acid digestion (Hydrofluoric (HF), Hydrochloric (HCl), Nitric (HNO_3), and Perchloric ($HClO_4$)) method defined by Garbe-Schonberg (1993) on each size fraction of the sediment samples (n = 126) (Section S2 in S.I.). Concentrations of sediment-borne As, Cu, Zn, Sn and Pb were determined using ICP-MS (Agilent 7700x), and Fe concentrations were determined using ICP-OES (Agilent 5110 VDV). Weighted averages of the concentrations of each size fraction based on their masses were calculated to represent the bulk composition of the samples. The Cu concentration at 5.88 km for >2 mm was taken from pXRF data due to a ten-fold overestimation in the ICP-MS data (See S3 for more details).

For estimation of the accuracy of the analysis, certified reference materials (RTS-3a, sulfide ore mill tailings; CANMET, stream sediments) were also run with the batch samples, along with the blanks and triplicates taken during sample preparation and field sampling (see S3 in S.I. for details) Accuracy was calculated as the coefficient of variation (CV %) between analysed and certified concentrations using Excel (2016) (see S3 in SI for CV % values). In addition, field sampling precision was calculated based on the triplicate sample taken during the campaign as CV%).

2.4. Mineralogical analysis

X-ray Diffraction analysis was completed on all samples (excluding input 5, see Table S1 in S.I.) using a Bruker D8 Advance XRD (CuKα radiation). Powder diffractograms were acquired in the 5–90° 2θ range, 1-s step, step size 0.03°2θ. Quantitative estimation of amorphous phase abundances using Rietveld refinement was not conducted in this study. Diffractogram interpretation was performed qualitatively with EVA v.18.0.0.0 software to identify crystalline mineral phases. Samples were prepared for XRD analysis by placing ~1 g of ground sample onto a microscope slide and flattening it with a spatula to give an even surface.

Morphological, and chemical and mineralogical compositions were determined for selected samples (n = 13) which exhibited high concentrations of As, Cu and Zn, which were near potential metal(loid) sources or were representative of up-, mid- or down-stream portions of the Carnon River catchment (see S1 in S.I.). The techniques used

included QEMSCAN® 4300 (Zeiss EVO 50 series SEM) and TESCAN VEGA3 GMU) automated mineralogical analysis. The QEMSCAN was operated at 24 kV and 5 nA beam using a tungsten filament. X-ray count was 1000 counts at a resolution of 0.3 μm from four EDS Bruker SDD detectors. A 10 μm X-ray pixel spacing resolution Fieldscan measurement mode was used. Data acquisition and spectral interpretation were carried out using iMeasure/iDiscover 4.2 SR1 and 5.3. The chemical data for each point were compared to the QEMSCAN library to assign a mineral identity. The abundances of each mineral were calculated with the iMeasure/iDiscover software and then portrayed on false colour plots and in and Excel database. SEM-EDS data acquisition was done using Aztec (V.3.3.) software. For sample preparation, one g of each dried sediment sample was mounted onto epoxy resin blocks (30 mm diameter), polished and then carbon coated (25 nm thickness).

Statistical analysis of all data was conducted with Origin Lab Pro using the Spearman's r correlation coefficient. The results presented had p-values <0.05.

3. Results and discussion

3.1. Weighted average sediment metal(loid) concentrations

Weighted average Carnon River sediment metal(loid) concentrations ranged from 1040 to 5040 mg/kg (Cu), 1460 to 8210 mg/kg (As), 56700 to 137000 mg/kg (Fe) and 478 to 2760 mg/kg (Zn) (Fig. 2) and were within range of those in other AMD-affected catchments (Table 1). The

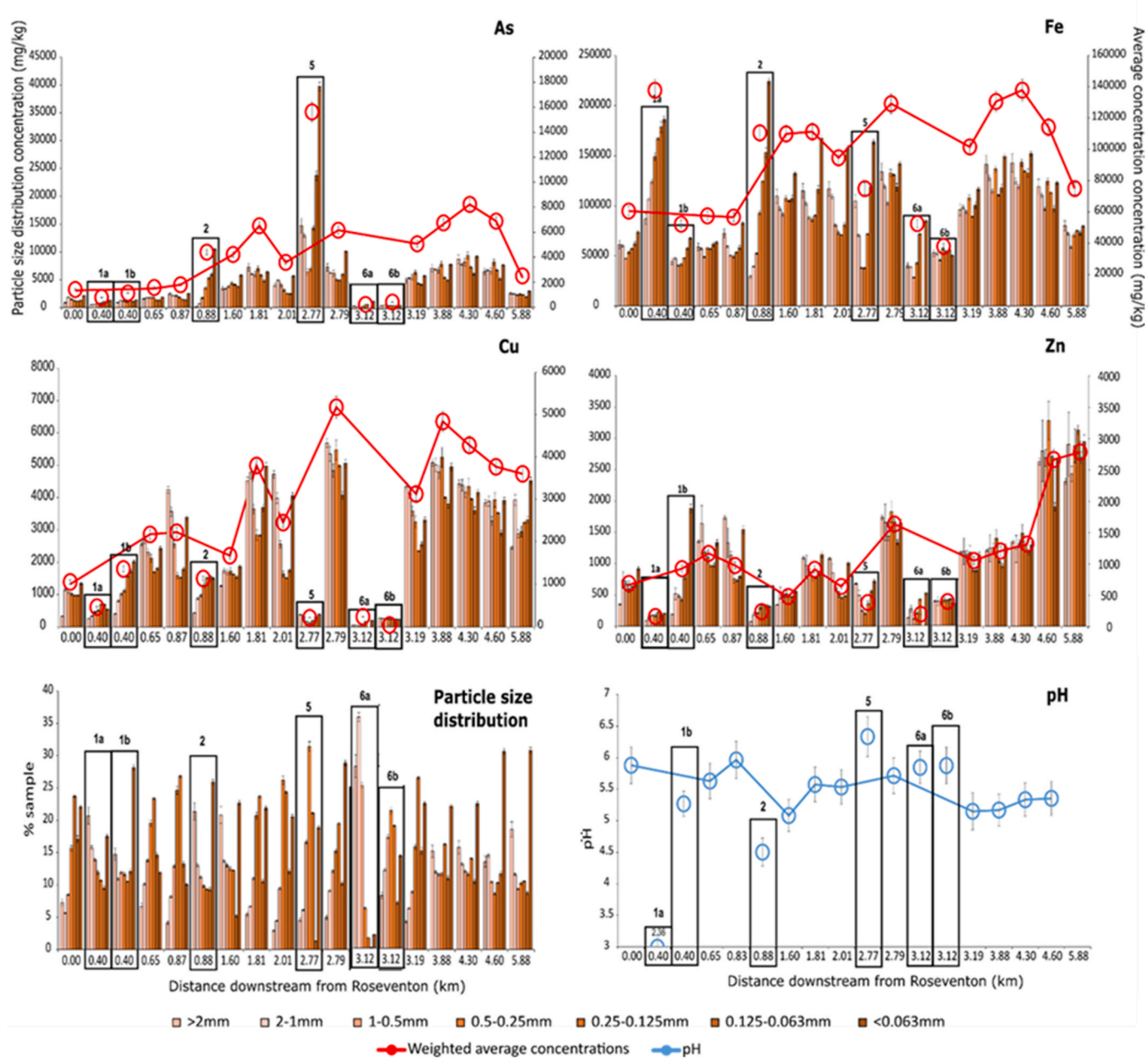

Fig. 2. Particle size distribution of As, Cu, Zn and Fe in Carnon river sediments plotted with weighted average concentrations (red scatter and line plot), Particle size % dominance (% mass retained) and pH vs distance downstream of Roseventon (0 km). Rectangle box plots highlight input sites. 0 km is a site upstream of the County Adit – Carnon River confluence (input 2, 0.88 km). Input 1 (a and b) is from Wheal Maid (0.4 km). Input 2 is the County Adit bank sediment (0.88 km). Input 5 is the potential Adit (2.77 km). Input 6 (a and b) is the Grenna Lane bridge stream (3.12 km). (For interpretation of the references to colour in this figure legend, the reader is referred to the Web version of this article.)

Table 1
River sediment metal(loid) concentrations in representative AMD-affected river systems. n.r. = not reported.

Element (mg/kg)	Site and study							
	Carnon River, Cornwall, UK n = 18 <2 mm		Zimpan, Mexico n = 14 <0.063 mm		Rio Pilcomayo, Bolivia n = 39 <2 mm		Rio Tinto, Spain n = 13 <2 mm	
	This study		Espinosa et al. (2009)		Hudson-Edwards et al. (2001)		Hudson-Edwards et al. (1999)	
	Min	Max	Min	Max	Min	Max	Min	Max
As	2550	8210	375	13600	5	7200	110	620
Cd	1.09	4.15	7	202	<0.5	190	n.r.	n.r.
Cu	1640	5040	n.r.	n.r.	9	1400	75	1500
Pb	185	396	202	4830	6	1700	490	7600
Zn	478	2760	299	19100	9	10000	26	1200

concentrations exceeded Environment Agency interim sediment quality guidelines (adopted from the Canadian sediment guidelines (CCME, 2001)) for the Threshold Effect Level (TEL) for As, Cu and Zn (S4 in S.I.) (Environment Agency, 2008; Hudson-Edwards et al., 2008). TEL represents the concentration that poses no major hazard to aquatic organisms. Very few samples had concentrations below the Potential Effect Level (PEL), the lower concentration limit for adverse biological effects (Environment Agency, 2008; Hudson-Edwards et al., 2008). Only sediment-borne Zn concentrations in the Wheal Maid culvert (input 1a, 0.4 km) (162 mg/kg) and the Grenna Lane Bridge channel sediment (input 6a, 3.12 km) (191 mg/kg) were below PEL guidelines for Zn (315 mg/kg) (Fig. 2, S4 in S.I.), and only the Grenna Lane Bridge channel sediment (input 6a, 3.12 km) (53.5 mg/kg) was below PEL guidelines for Cu (197 mg/kg) (Fig. 2, S4 in S.I.). The elevated sediment metal(loid) concentrations downstream in the Carnon River in comparison to environmental guidelines and their comparable concentrations to other AMD-affected river systems highlights the ongoing contamination in the area and limited natural attenuation. While metal(loid) precipitation and sedimentation act as natural attenuation processes by removing metals from the water column, these processes promote the accumulation of metal(loid)s in sediments. As such, sediments represent a secondary source of contamination, where stored metals may be remobilised under changing environmental conditions (e.g., variations in pH, redox conditions, or physical disturbance) as oberseved by Jarvis et al. (2019). The Carnon River sediments also exhibit a higher minimal As, Cu and Zn concentrations than those from representative global AMD-affected rivers (Table 1), further supporting the persistence of contamination despite mining ceasing in 1991 at Wheal Jane.

The aqueous pH in the Carnon River upstream of the County Adit – Carnon River confluence (0 to 0.87 km) was 5.6-6 and decreased from

Table 2
Sediment mineralogy determined by XRD in the Carnon River and other AMD-affected rivers.

Mineral	Mineral group	Carnon River, Cornwall This study	Zimapan, Mexico (Espinosa et al., 2009)	Rio Pilcomayo, Bolivia (Hudson-Edwards et al., 2001)	Rio Tinto, Spain (Hudson-Edwards et al., 1999)	Tibetan Plateau, China (Ye et al., 2022)
Albite ($NaAlSi_3O_8$)	Feldspar	x				x
Anglesite ($PbSO_4$)	Sulfates	x				
Azurite ($Cu_3(CO_3)_2(OH)_2$)	Carbonates	x				
Baryte ($BaSO_4$)	Sulfates	x			x	
Biotite ($K(Mg,Fe)_3AlSi_3O_{10}(F,OH)_2$)	Phyllosilicates	x				
Cassiterite (SnO_2)	Oxides	x		x		
Cerussite ($PbCO_3$)	Aragonite	x				
Chlorite ($(Al, Fe^{2+}, Fe^{3+}, Li, Mg, Mn, Ni)_{5\text{-}6}(Al, Fe^{3+})_4(O,OH)_{18}$)	Phyllosilicates	x			x	
Clinochlore ($Mg_5Al(AlSi_3O_{10})(OH)_8$)	Phyllosilicates	x				
Diaspore (AlO(OH))	Oxide	x				
Goethite (FeO_2H)	Oxide	x			x	
Gypsum ($CaSO_4{\cdot}2H_2O$)	Sulfates	x	x	x	x	x
Hemimorphite ($Zn_4(Si_2O_7)(OH)_2{\cdot}H_2O$)	Silicates	x				
Illite ($K_{0.6\text{-}0.85}(Al,Mg,Fe^{2+})_2(Si,Al)_4O_{10}(OH)_2$)	Phyllosilicates	x		x	x	
Jarosite ($KFe_3^{3+}(SO_4)_2(OH)_6$)	Alunite	x	x		x	
Kaolinite ($Al_2O_32SiO_2{\cdot}2H_2O$)	Silicates	x	x			
Magnetoplumbite ($Pb^{2+}Fe_{12}^{3+}O_{19}$)	Oxides	x				
Malachite ($Cu_2CO_3(OH)_2$)	Carbonate	x				
Montmorillonite ($(OH)_4Si_8Al_4O_{20}{\cdot}nH_2O$)	Phyllosilicates	x	x			
Muscovite ($KAl_2(AlSi_3O_{10})(OH)_2$	Phyllosilicates	x	x			x
Natrojarosite ($NaFe_3(SO_4)_2(OH)_6$)	Alunite	x			x	
Parascorodite ($FeAsO_4 \cdot 2H_2O$)	Arsenates	x				x
Pyromorphite ($Pb_5(PO_4)_3Cl$)	Phosphate	x				
Quartz (SiO_2)	Silicates	x	x	x	x	x
Rosasite ($(Cu,Zn)_2(CO_3)(OH)_2$)	Carbonate	x				
Schorl ($NaFe_3^{2+}Al_6(Si_6O_{18})(BO_3)_3(OH)_3(OH)$)	Silicates	x				
Scorodite ($FeAsO_4{\cdot}2H_2O$)	Arsenates	x			x	
Woodruffite ($Zn^{2+}_{\sim 0.4/2}(Mn^{4+}_{1\text{-}\sim 0.4}Mn^{3+}_{\sim 0.4})O_2 \cdot {}_{\sim 0.7}H_2O$)	Oxides	x				

the mixing with the AMD County Adit (pH 4.5, input 2, 0.88 km) to 5.08 downstream of the County Adit – Carnon River confluence (1.6 km) (Fig. 2). The pH then increased downstream at 1.81 km and remained at 5.5-5.7 to 2.79 km (Fig. 2). After 2.79 km, the pH decreased to 5.2 at 3.19 km and increased towards the brackish water (4.6 km) to 5.3 (Fig. 2). These downstream changes in pH likely influenced the formation of secondary minerals and metal(loid) partitioning into the sediments.

3.2. Metal(loid)-bearing minerals

The main Carnon River sediment-borne mineral hosts for As, Cu and Zn that were determined by XRD included Fe oxides, arsenates, sulfides and alunites. These have been documented in other AMD-affected catchments, such as the Rio Tinto (Spain) and Zimapán (Mexico) (Hudson-Edwards et al., 1999; Espinosa et al., 2009) (Table 2). Overall, the XRD mineral assemblage is dominated by silicate phases (quartz, feldspars and phyllosilicates), with secondary Fe-bearing minerals (Fe oxides and oxyhydroxysulfates such as jarosite and natrojarosite), arsenates (e.g. scorodite) and minor sulfides and carbonates (S5).

The contaminant hosting phases decreased in the order Fe oxides (average 6 vol %) > arsenates (average 0.21 vol %, including arseniosiderite/kolfanite, bukovskyite, pharmacosiderite and scorodite) > sulfides (average 0.16 vol %, including altered pyrite, chalcopyrite, pyrite and sphalerite) > jarosite (average 0.18 vol %) in the sediment samples from the Carnon River (Table 3). The 'altered pyrite' (average 0.57 vol %) identified with QEMSCAN may have been jarosite, Fe oxide or another secondary Fe ± S ± O phase (Table 3).

The QEMSCAN chemical analysis suggested that As occurred in scorodite, arseniosiderite/kolfanite, bukovskyite, pharmacosiderite, sphalerite, altered pyrite, jarosite, and Fe oxides (Table 3). Weighted average sediment-borne As concentrations were positively correlated with bulk Fe concentrations at all corresponding particle sizes ($r = 0.832$-0.93, degrees of freedom (df) $= 20$, p value < 0.01) and with Fe oxides ($r = 0.627$-0.827, df $= 20$, p value < 0.05) (Figs. 2 and 5, S6 in SI). Scorodite also positively correlated with As in all particle sizes ($r = 0.645$-0.79, df $= 20$, p value < 0.05) (Fig. 4). However, the volume % of the scorodite was low and its correlation with As may not have contributed to the positive weighted average sediment As–Fe correlation (Fig. 4).

The SEM-EDS analysis suggested that Cu was hosted in phases such as altered pyrite, chalcopyrite, jarosite, and Fe oxides (identified with QEMSCAN mineral chemistry) (Table 3). Weighted average concentrations of Cu and Fe did not correlate (S6 in SI). However, only the coarser particle size (>2 mm −1 mm) concentrations of Fe correlated with all the particle size concentrations of Cu ($r = 0.643$-0.776, df $= 20$, p value < 0.05) (Fig. 2), suggesting that chalcopyrite (Fig. 3), Cu-bearing Fe oxides or Cu-bearing pyrite (Table 3) were the dominant Cu hosts in these grains.

Zinc was suggested by SEM-EDS analysis to occur in sphalerite, jarosite, altered pyrite and Fe oxides in the Carnon River sediments (identified with QEMSCAN mineral chemistry) (Table 3). The weighted average Zn concentrations and the individual particle size Zn concentrations did not correlate with those of Fe, suggesting that the Fe oxides were not primary hosts of Zn (Fig. 3, S6 in SI). Sediment-borne Zn concentrations in all particle sizes correlated with vol % of sphalerite, Cu sulfide and chalcopyrite ($r = 0.636$-0.8, df $= 20$, p value < 0.05 (excluding Zn at 2-1 mm for sphalerite), suggesting that these minerals may instead have been the dominant hosts of Zn.

Amalgamated particles ranging from 0.25 to 1 mm with rounded to angular shapes were documented using SEM and QEMSCAN in the Carnon River sediments (Fig. 3). These particles consisted of clay minerals, chlorite, quartz with metal(loid) phases such as pyrite, altered pyrite, sphalerite, chalcopyrite, and Fe oxides (Fig. 3, S5 in S.I., formulas in Tables 2 and 3).

3.3. Downstream patterns of sediment-borne metal(loid) concentrations and mineralogical abundances

Unlike other mining-affected river systems, in which sediment-borne metal(loid) concentrations decrease downstream of sources or due to dilution from tributaries (Hudson-Edwards et al., 2003; Macklin et al., 2006), the Carnon River sediment concentrations increased downstream from 0 km to the estuary (5.88 km) (Fig. 2). This unusual increase underscores the continual remobilisation of legacy mine waste and deposition of AMD-generated metal(loid)s, potentially preventing natural attenuation.

The downstream patterns of Fe and As concentrations showed a broadly similar trajectory, with both increasing shortly after the source, remaining elevated from 0.89 to 4.3 km, and declining towards the estuary (5.88 km) (Fig. 2). This trend was reflected in the abundance of Fe-oxide phases, including oxides and oxyhydroxysulfates, which increased notably at the County Adit – Carnon River confluence (0.89 km), remained relatively consistent until around 4.3 km, and declined to the estuary (Fig. 4). Scorodite followed a trend similar to Fe-oxides and As, increasing downstream of the County Adit confluence, with peaks at 1.81 km and 4.3 km, before decreasing towards the estuary (Figs. 2 and 5). These matching trends highlight the likelihood of secondary precipitation driving sediment-borne As enrichment.

Pyrite, altered pyrite, and jarosite also showed broadly similar downstream trends (Fig. 4). The abundances of all three increased at 0.88 km, fluctuated downstream and increased in the brackish section of the river (4.6 km) (Fig. 4). Jarosite and altered pyrite abundances increased downstream of the Carnon River – County Adit confluence (0.89 km), with jarosite peaking at 4.6 km (Fig. 4). These trends suggest in situ weathering and mineral transformation during transport.

Weighted average copper and Zn concentrations and chalcopyrite, sphalerite, and bukovskyite abudances increased with distance downstream (Fig. 2). Chalcopyrite abundance increased slightly at 0.87 km, decreased at 1.6 km, then increased downstream, with a notable rise in the estuarine sediments (5.88 km) (Fig. 4). Sphalerite abundance remained low until 4.3 km, increasing slightly at the estuary (Fig. 4).

Table 3
Average volume % of metal(loid) bearing minerals identified with QEMSCAN and SEM-EDS for sediment samples from the Carnon River ($n = 11$)[1], its tributaries and inputs ($n = 2$, the County Adit (input 2, 0.88 km) and the potential Adit (input 5, 2.77 km)[2]. Volume % was calculated using QEMSCAN data.

Mineral	Mineral Chemistry	vol. % [1]	vol. % [2]	As	Cu	Zn	Fe
Altered Pyrite (FeS (may include other trace elements))	Fe S O (+trace elements)	0.53	1.2	X	X	X	X
Arseniosiderite/Kolfanite ($Ca_2Fe^{+3}_3(AsO_4)3O_2{\cdot}3H_2O$/$Ca_2Fe^{+3}_3O_2(AsO_4)_3 \cdot 2H_2O$)	As, Fe, Ca, O	0.01	5.8	X			
Bukovskyite ($Fe_2(AsO_4)$ (SO_4) $(OH){\cdot}7H_2O$)	As, Fe, S, O	0.02	0.13	X			X
Chalcopyrite ($CuFeS_2$)	Fe, Cu, S (+bornite (Cu_5FeS_4))	0.1	<0.01		X		
Iron oxides	Fe, O, H (trace elements)	6	19.4	X	X	X	X
Jarosite ($KFe^{3+}_3(SO_4)_2(OH)_6$ (may include altered Pyrite))	Fe, S, O, K, H (+altered pyrite)	0.18	0.1	X	X	X	X
Pharmacosiderite ($KFe_4(AsO_4)_3(OH)_4{\cdot}$ (6-7) H_2O)	Fe, As, K, O, H	<0.01	0.263	X			X
Pyrite (FeS_2)	Fe, S	0.02	0.2				X
Scorodite ($FeAsO_4{\cdot}2H_2O$)	As, Fe, O	0.17	8	X			X
Sphalerite (ZnS)	Zn, S (minor Fe + Mn)	0.02	<0.01			X	

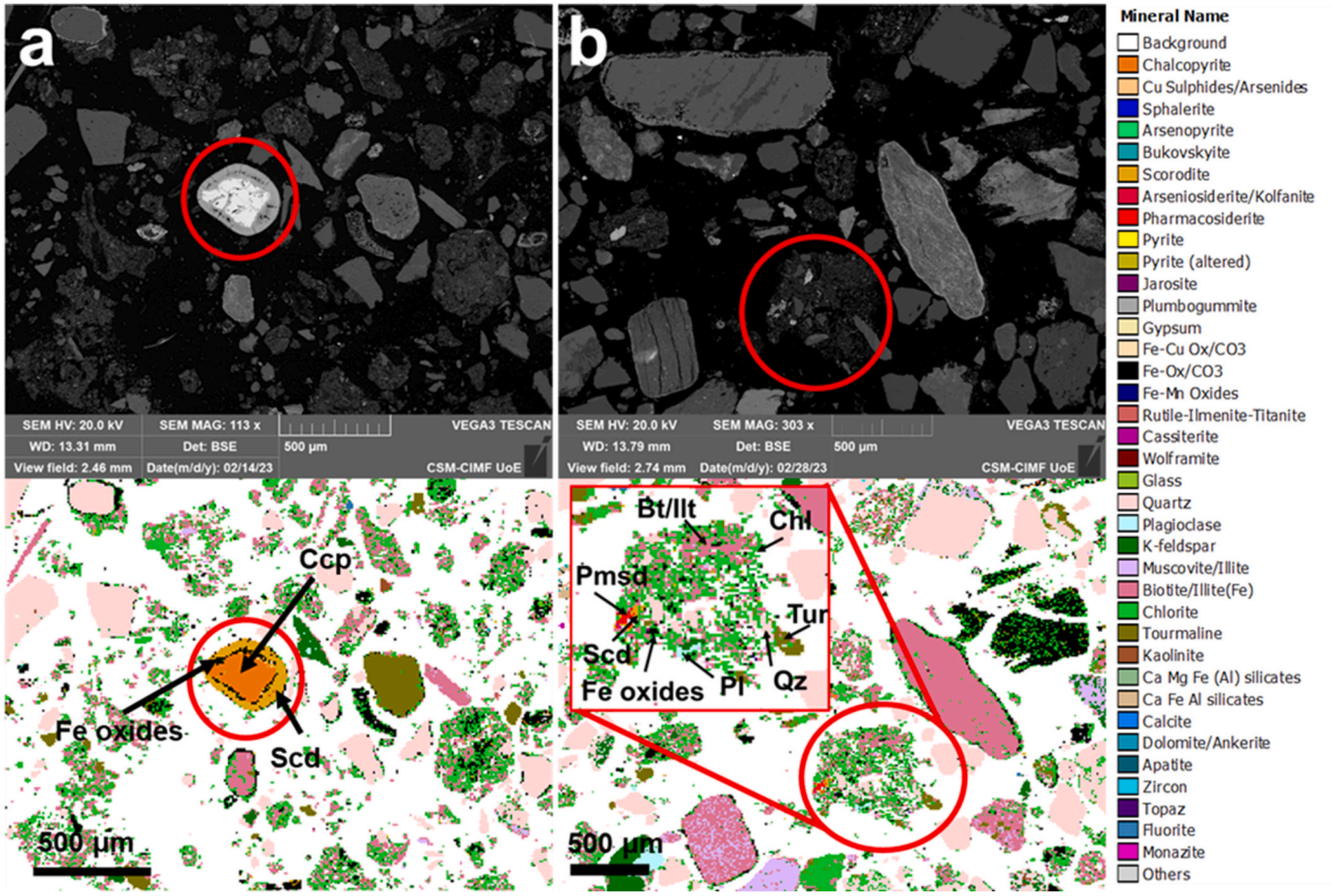

Fig. 3. Back-scattered electron images of polished sections and automated mineralogy (QEMSCAN) of samples taken in the Carnon River. Red circle highlights the grain of interest where chalcopyrite is in the centre (orange) with scorodite, and Fe oxides precipitated around the grain found at the brackish water entry (4.3 km). B) Is an example of an amalgamated particle found in the Carnon River (this grain was taken at 1.81 km downstream of input 3, Fig. 1). Mineral abbreviations taken from Warr (2021) excluding altered pyrite and Fe oxides. Chlorite 'Chl', tourmaline 'Tur', quartz 'Qz', chalcopyrite 'Ccp', plagioclase 'Pl', biotite/illite 'Bt/Ilt', pharmacosiderite 'Pmsd', and scorodite 'Scd'. (For interpretation of the references to colour in this figure legend, the reader is referred to the Web version of this article.)

Bukovskyite showed a stepped pattern, with increases at 0.87 km, 2.01 km, and 5.88 km (Fig. 4). Arseniosiderite/kolfanite and pharmacosiderite increased slightly downstream of the County Adit – Carnon River confluence (0.89 km) (Fig. 4).

All of the downstream metal(loid) increases in the freshwater sediments of the Carnon River were likely driven by both the ongoing transport of 'detrital' (pyrite, chalcopyrite, sphalerite) sulfides and the formation of Fe- and S- bearing secondary minerals (Fe oxides and jarosite). In the estuarine sediments, the reducing conditions may also facilitate the formation of secondary sulfides, consistent with the high pyrite abundances observed in these samples (Fig. 4). These processes highlight the limited attenuation occurring in the Carnon River.

3.4. Sediment particle size and metal(loid) concentration distributions

The dominant particle size of the Carnon River sediments was <0.5 mm (maximum total sample mass retained of 31 %), up until ~3.19 km with a few exceptions, including 1.6 km where >2 mm was dominant, with a mass retention of 20.8 % of the overall sample mass (Fig. 2). In river systems underlain by silt- and sandstones, such as the Carnon River, it can be assumed that riverine sediments would be dominated by finer silt to sand size particles <2 mm. However, factors such as river flow dynamics, sediment supply, and catchment hydrology can influence particle size distribution (Bouchez et al., 2011), making comparisons to catchments with similar geology challenging. The finer particle dominance in the Carnon River can be attributed to the presence of Fe oxides and oxyhydroxysulfates ochres that form downstream of the County Adit – Carnon River confluence (0.89 km) and are transported, deposited and easily remobilised during physical disturbance (Jennings et al., 2025), or to inputs of mine tailings during historic mining. The presence of detrital ore material as seen in Fig. 3 (chalcopyrite) could support this mine waste deposition. The >2 mm particles observed could be due to agglomeration of the ochres or to mobilisation of coarser particle mine waste from the legacy mine sites such as Wheal Busy (N 50.259, W −5.176), Wheal Virgin (N 50.236, W −5.163) and Wheal Peevor (N 50.253, W −5.217) (Buckley, 1992).

Throughout the Carnon River, there was no consistent relationship between particle size and metal(loid) concentration (Fig. 2). However, a bimodal pattern existed for Cu, Fe and Zn at sites 0.87 km, 1.81 km, and 2.01 km (Fig. 2). Here, the >2 mm and <0.063 mm particle sizes had high concentrations of As, Cu, Fe and Zn, whereas the 0.5 to 0.125 mm particle sizes had the lowest concentrations (Fig. 2). This suggests that there were two metal(loid) bearing phases displaying opposite trends, one a direct relationship (increasing concentration with increasing particle size) and the other an inverse relationship (increasing concentration with decreasing particle size).

Indirect relationships highlight that metal(loid) concentrations increased in finer particle sizes. This could be due to the insolubility of metal(loid)-bearing phases that caused them to persist during physical and chemical weathering (Kim et al., 2011). Alternatively, the metal

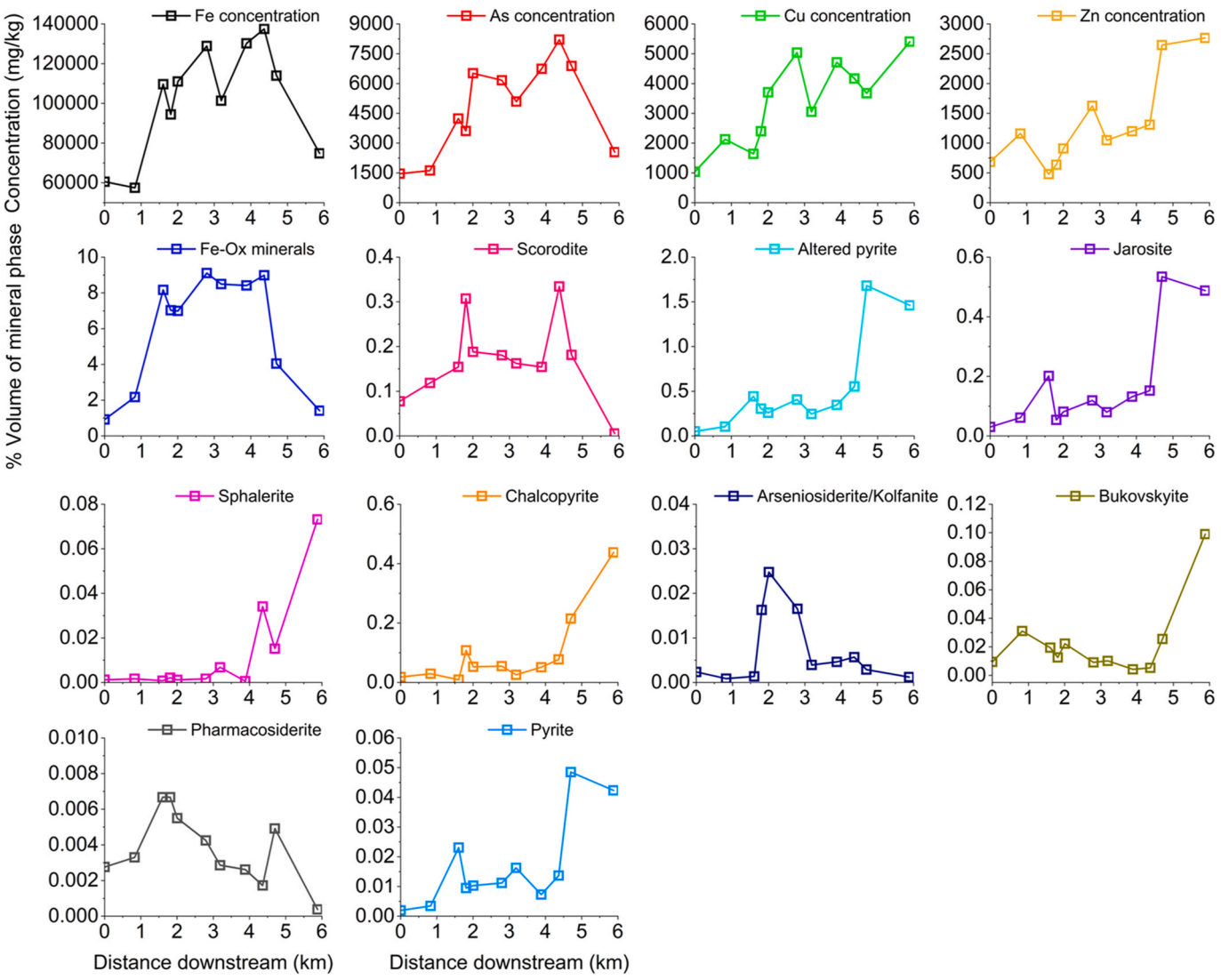

Fig. 4. Weighted average sediment-borne concentrations of Fe, Cu, As and Zn (mg/kg) and host metal(loid) minerals (see Table 3 for relevant mineral source for the metal(loid)s) (volume % mineral measured using QEMSCAN) as a function of distance downstream from Roseventon (0 km) in the Carnon River sediments. 0 km is a site upstream of the County Adit – Carnon River confluence (input 2, 0.89 km).

(loid)s may have been sorbed species on minerals such as Fe oxides and oxyhydroxysulfates, where the proportion and surface area for the species increase as particle size decreases (Kim et al., 2011).

Iron and As concentrations did not vary downstream in the particle sizes and were found to be most concentrated in the finest particle size <0.063 mm (Fig. 2). Initially, the finest particle sizes were the most concentrated in Cu and Zn from 0 to 2.01 km, after which >2 mm and 0.5-0.25 mm particle sizes till the brackish water (4.6 km) (Fig. 2). At the brackish water the finer particle sizes became more concentrated in Cu and Zn (Fig. 2).

These results highlight that metal(loid) enrichment is likely particle-size dependent, with As largely stored in fine Fe-rich particles (<0.5 mm) and Cu–Zn partitioned between fine sorbed phases (<0.5 mm) and coarser fragments (>0.5 mm) (Fig. 2).

3.5. Geochemical, mineralogical and particle-size controls on the origin, transport and storage of sediment-associated metal(loid)s in the Carnon River

The downstream patterns and particle-size sediment metal(loid) concentration data and their downstream patterns, and mineralogical textures were used to discern the origins and sources of As, Cu and Zn in the Carnon River catchment. The predominance of fine particles (<0.5 mm) in the upstream and midstream reaches (Fig. 2) likely reflects the occurrence of As-, Cu- and Zn-bearing Fe oxide ochres that were generated at the County Adit-Carnon River confluence (Jennings et al., 2025). By contrast, notable enrichment of Cu and Zn in coarse fractions (>2 mm) (Fig. 2) can be related to the presence of less-weathered sulfide fragments (Fig. 3, chalcopyrite) and aggregate Cu- and Zn-bearing grains (Fig. 3). This dual distribution across particle sizes suggests different transport and weathering mechanisms for Fe–As and Cu–Zn. Therefore, the metal(loid)s analysed in this study can be divided into two groups (As–Fe and Cu–Zn) based on their occurrence and behaviour in the Carnon River sediments.

The mineralogical diversity observed reflects spatially variable redox conditions, pH gradients, and ionic strength variations across the Carnon River catchment. Such geochemical heterogeneity directly governs the mobility, bioavailability, and stability of As, Cu, and Zn in riverine sediments. The co-occurrence of primary sulfides (e.g., pyrite, arsenopyrite, chalcopyrite, sphalerite) with secondary weathering products (e.g., Fe oxides, jarosite, scorodite) indicates ongoing metal(loid) cycling and transformation (Fig. 4, Tables 2 and 3). Downstream distributions of metal(loid)s and their mineral hosts further suggest that these contaminants are subject to remobilisation and redistribution.

Remobilisation is likely driven by dynamic geochemical shifts, particularly pH changes (Equeenuddin et al., 2013), redox (Lynch et al., 2014), and ionic strength (Millward, 1995; Braungardt et al., 2003; Lynch et al., 2014). Physical transport mechanisms, including bank erosion and sediment resuspension (Foulds et al., 2012), also contribute to redistribution, particularly in mid-reach zones (3.19–4.3 km) where flocculation and secondary mineral precipitation are enhanced by mixing of acidic and circumneutral waters.

Downstream enrichment in Cu and Zn, particularly between 4.3 and 5.88 km (Fig. 2), reflect continued transport and weathering of sulfide phases, primarily chalcopyrite and sphalerite (Figs. 3 and 5). These trends were accompanied by increases in jarosite and altered pyrite (Fig. 4), pointing to in situ transformation of primary sulfide minerals. The persistence of these phases downstream (Fig. 4) suggests that these primary grains remained active sources of Cu and Zn over extended periods, likely dating back to at least the last mine (Wheal Jane) closure in the catchment in 1991 (Buckley, 1992; Pirrie et al., 2003; Neal et al., 2005; Rainbow, 2020). While Zn exhibited a significant positive relationship with sphalerite ($r = 0.6$-0.8, $df = 20$, $p < 0.05$), Cu did not show a significant correlation with chalcopyrite. This may indicate that factors such as differential weathering rates or transport mechanisms influenced the Cu distribution downstream. Additional targeted evidence would be required to conclusively identify the dominant source.

Arsenic and Fe exhibited a significant positive correlation in all particle sizes, with peak concentrations at 4.3 km, followed by a decline near the estuary (Fig. 2). This spatial pattern coincided with increased abundances of Fe oxides and arsenate minerals (e.g., scorodite, arseniosiderite) (Fig. 4), indicative of secondary mineral precipitation, highlighting the importance of these minerals in As sequestration. These Fe oxide phases likely formed through secondary precipitation from the County Adit, where Fe(II) was oxidised and hydrolysed precipitating Fe oxides (Jennings et al., 2025). These Fe oxides have the potential to co-precipitate or sorb As, Cu and Zn, transporting them further downstream as suspended particulates (Fig. 3; Jennings et al., 2025), further highlighting their role in the transport and storage of As, Cu and Zn in the Carnon River catchment.

The affinity for cations and anions for sorption onto Fe oxides can change with pH (Dzombak and Francois, 1990; Wołowiec et al., 2019). At lower pH, there are higher concentrations of H^+ ions that will cause protonation of the Fe oxide surface (Dzombak and Francois, 1990; Wołowiec et al., 2019) giving a positive zeta potential (ζ) surface charge. This can result in the attraction ofanions such as arsenate and arsenite to the Fe oxide surface (Dzombak and Francois, 1990; Wołowiec et al., 2019). This is reflected in the observed enrichment of As in fine Fe oxide-bearing particles downstream of the County Adit – Carnon River Confluence, where the pH was ~5.

Redox-transitional zones emerge along metal(loid)-contaminated riverbanks, experiencing alternating wetting and drying cycles due to flooding and drought (Byrne et al., 2013; Lynch et al., 2014), these zones are likely prominent at the lower end of the Carnon River near the brackish water entry (4.6 km), from the tidal influences. These fluctuations alter the redox potential, modifying the composition of mine waste through the dissolution or precipitation of iron, manganese, sulfide, and sulfate minerals (Byrne et al., 2013; Lynch et al., 2014). This in turn results in the release or uptake of associated contaminants in the mine waste (Lynch et al., 2014). Lateral infiltration from flooded river sediments also introduces dissolved organic carbon, escalating microbial activity and depleting oxygen creating reducing conditions (Lynch et al., 2014). Under these conditions, reductive dissolution of Fe can occur through electron transfer from organic matter or a reduced metal (loid) as an electron donor, releasing ferrous Fe and, consequently, associated co-precipitated contaminants (Lynch et al., 2014). The downstream enrichment of Zn, Cu, and As in sediments observed in this study (Fig. 2) could be due to these processes. Reducing conditions caused by flooding of river embankments and floodplains may lead to sulfate reduction to H_2S (Lynch et al., 2014), which is consistent with the observed increase in riverine pH at input 5 (wetlands) (Fig. 2). The behaviour of aqueous S governed by factors such as redox, reported by Jennings et al. (2025) supports the role of redox-controlled S cycling in regulating metal mobility in such systems. H_2S reacts readily with dissolved contaminants, precipitating metal sulfides and H+ ions (Equation (1.9)) (Lynch et al., 2014). These can be taken up by co-precipitation on iron or metal sulfides, such as ZnS, PbS, and CuS (Lynch et al., 2014). Iron and metal(loid) sulfides undergo oxidation, generating AMD and releasing co-precipitated contaminants. While the oxidation of metal monosulfides does not increase acidity, hydrolysis can produce H+ ions, leading to acidic conditions (Lynch et al., 2014). The observed downstream increase in sulfides (Fig. 4) suggests that these processes occurred in the Carnon River, facilitating the sequestration of Zn, Cu, and As through co-precipitation or incorporation into these minerals. However, this could also be related to the mobilisation of eroded mine waste, containing ore minerals such as chalcopyrite, sphalerite and pyrite observed in Figs. 3 and 4, potentially from mine sites listed in Fig. 1.

Projected climate change could amplify these processes. Future changes in river discharge globally are predicted to become irregular with extreme weather events due to climate change (Arnell and Gosling, 2013; Arnell et al., 2015). High river discharge can increase the rate of metal(loid) mobilisation due to erosional (physical entrainment; dissolution of Fe oxides (Byrne et al., 2013) and chemical processes (decreasing pH from increased run off from acid sources such as peat soils (Jarvis et al., 2019)). Lower discharges can also have indirect detrimental effects, such as increasing metal(loid) loads by promoting accumulation and enrichment in sediment-bound phases (Byrne et al., 2020). In the future, high-discharge events are expected to become more frequent (Byrne et al., 2013), and the Carnon River is no exception, with long-term flood risk maps (GOV UK, 2025) predicting an increased likelihood of annual flooding and its severity. Altogether, these shifts could drive the Carnon River towards increasingly episodic or even chronic contaminant mobilisation.

All of the findings of this study underscore the importance of both particle size and mineralogy in understanding sediment-associated metal(loid) transport. Improved understanding of these controls is critical for assessing contaminant fluxes, predicting remobilisation risks, and informing targeted remediation strategies in historically mined river systems. This is particularly important in estuarine environments, where metal(loid)s may be preferentially retained in solid phases and therefore not fully captured by aqueous phase analysis alone.

4. Conclusions

This study demonstrated how particle size and mineralogical associations control the distribution, storage and mobility of As, Cu and Zn in the Carnon River, a historically contaminated, AMD-impacted river system. Sediment concentrations of As, Cu, Zn, and Fe remained elevated downstream of a major AMD input (input 2, 0.88 km), and high sediment concentrations have been recorded in the estuary (5.88 km): As (2550 mg/kg), Cu (3510 mg/kg), Zn (2760 mg/kg), and Fe (74,900 mg/kg). This in contrast to other typical AMD impacted river systems where concentrations are expected to decrease due to increased distance from their source, natural attenuation via co-precipitation and sorption or via dilution from inputting 'clean' tributaries (e.g. the Jiehe River, China (Zhang et al., 2014), and the Hengshi River, China (Wei et al., 2022)). Within this the fine (<0.063 mm) and coarse (>2 mm) sediment fractions exhibited elevated concentrations of metal(loid)s, suggesting two discrete mechanisms of contaminant accumulation.

Such fine-grained sediments were enriched in Fe oxides, which acted as dominant hosts for As and Cu, likely due to their adsorption and/or co-precipitation. These secondary phases, which formed downstream of the AMD input, were susceptible to geochemical remobilisation under fluctuating redox and flow conditions. In contrast, the coarse sediment fraction was characterised as containing detrital sulfide minerals, particularly chalcopyrite and sphalerite, which suggests that they

originated from the direct deposition of mine waste, and were unrelated to the AMD input. The occurrence of these grains at both upstream and downstream sites suggests that they were widely deposited, highlighting continued mine waste input, sediment transport and physical reworking.

Zinc was primarily associated with sulfide and sulfate phases, while the co-occurrence of As and Fe in fine fractions suggests precipitation of arsenate and Fe oxide phases. Notably, the estuarine zone represented a significant sink for fine particles and associated contaminants, where elevated ionic strength likely promoted metal(loid) precipitation and long-term sediment accumulation. This work reveals that aqueous phase analyses alone may not reveal the potentially significant impacts of legacy mining contamination on these estuarine waters, which are a major sink for solid phase metal(loids).

These findings demonstrate the controls on partitioning between aqueous and solid phases within riverine systems, and specifically how the physico-chemical characteristics of sediments control the fate of metal(loid)s within AMD-affected catchments. The presence of contaminant metal(loid)s in both fine and coarse sediment fractions indicates pervasive and persistent contamination, increasing the potential for both long-term storage and episodic remobilisation during high-flow events. This underscores the need for catchment-scale management strategies that extend beyond remediation focused solely on fine sediments. By distinguishing between different sources and deposition processes of contaminants in mining-affected river systems, this work highlights a critical consideration for designing effective management interventions.

CRediT authorship contribution statement

Elin Jennings: Conceptualization, Data curation, Formal analysis, Methodology, Writing – original draft, Writing – review & editing. **Patrizia Onnis:** Conceptualization, Data curation, Formal analysis, Writing – review & editing. **Rich Crane:** Conceptualization, Data curation, Formal analysis, Writing – review & editing. **William M. Mayes:** Writing – review & editing. **Adam P. Jarvis:** Writing – review & editing. **Karen A. Hudson-Edwards:** Conceptualization, Data curation, Formal analysis, Writing – review & editing.

Declaration of competing interest

The authors declare that they have no known competing financial interests or personal relationships that could have appeared to influence the work reported in this paper.

Acknowledgements

The authors acknowledge the UK Natural Environment Research Council for funding (grant no. NE/T003022/1, Legacy Wastes in the Coastal Zone: Environmental Risks and Management Futures) and the University of Exeter for a PhD studentship for E.J. The authors thank Sharon Uren and Gavyn Rollinson from the University of Exeter for providing chemical and mineralogical analysis and the EM3 research group, University of Exeter, for assistance with fieldwork.

Appendix A. Supplementary data

Supplementary data to this article can be found online at https://doi.org/10.1016/j.apgeochem.2026.106859.

Data availability

Data will be made available on request.

References

Akcil, A., Koldas, S., 2006. Acid mine drainage (AMD): causes, treatment and case studies. J. Clean. Prod. 14 (12–13), 1139–1145. https://doi.org/10.1016/J.JCLEPRO.2004.09.006.

Arnell, N.W., Halliday, S.J., Battarbee, R.W., Skeffington, R.A., Wade, A.J., 2015. The implications of climate change for the water environment in England. Prog. Phys. Geogr. Earth Environ. 39 (1), 93–120. https://doi.org/10.1177/0309133314560369.

Arnell, N.W., Gosling, S.N., 2013. The impacts of climate change on river flow regimes at the global scale. J. Hydrol. 486, 351–364. https://doi.org/10.1016/j.jhydrol.2013.02.010.

Banks, D., Younger, P.L., Arnesen, R.T., Iversen, E.R., Banks, S.B., 1997. Mine-water chemistry: the good, the bad and the ugly. Environ. Geol. 32 (3), 157–174. https://doi.org/10.1007/s002540050204.

Bouchez, J., Gaillardet, J., France-Lanord, C., Maurice, L., Dutra-Maia, P., 2011. Grain size control of river suspended sediment geochemistry: clues from amazon river depth profiles. G-cubed 12 (3). https://doi.org/10.1029/2010GC003380.

Braungardt, C.B., Achterberg, E.P., Elbaz-Poulichet, F., Morley, N.H., 2003. Metal geochemistry in a mine-polluted estuarine system in Spain. Appl. Geochem. 18 (11), 1757–1771. https://doi.org/10.1016/S0883-2927(03)00079-9.

Bryan, G., Gibbs, P., 1983. Heavy metals in the Fal estuary, Cornwall: a study of long term contamination by mining waste and its effects on estuarine organisms. *Marine Biological Association* [Preprint]. http://plymsea.ac.uk/275/. (Accessed 17 February 2021).

BSI, 2020. BS ISO 11277:2020 soil quality. Determination of particle size distribution in mineral soil material. Method by sieving and sedimentation. https://bsol-bsigroup-com.uoelibrary.idm.oclc.org/Bibliographic/BibliographicInfoData/000000000030332192. (Accessed 20 January 2021).

Buckley, 1992. The Cornish Mining Industry: a Brief History. Tor Mark Press, Accessed. https://scholar.google.co.uk/scholar?hl=en&as_sdt=0%2C5&q=The+Cornish+mining+industry%3A+a+brief+history&btnG=. (Accessed 19 November 2020).

Butler, B.A., 2009. Effect of pH, ionic strength, dissolved organic carbon, time, and particle size on metals release from mine drainage impacted streambed sediments. Water Res. 43 (5), 1392–1402. https://doi.org/10.1016/j.watres.2008.12.009.

Byrne, P., Onnis, P., Runkel, R.L., Frau, I., Lynch, S.F.L., Edwards, P., 2020. Critical shifts in trace metal transport and remediation performance under future low river flows. Environ. Sci. Technol. 54 (24), 15742–15750. https://doi.org/10.1021/acs.est.0c04016.

Byrne, P., Reid, I., Wood, P.J., 2013. Stormflow hydrochemistry of a river draining an abandoned metal mine: the Afon Twymyn, central Wales. Environ. Monit. Assess. 185 (3), 2817–2832. https://doi.org/10.1007/s10661-012-2751-5.

Casiot, C., Lebrun, S., Morin, G., Bruneel, O., Personné, J.C., Elbaz-Poulichet, F., 2005. Sorption and redox processes controlling arsenic fate and transport in a stream impacted by acid mine drainage. Sci. Total Environ. 347 (1–3), 122–130. https://doi.org/10.1016/j.scitotenv.2004.12.039.

CCME, 2001. Canadian sediment quality guidelines for the protection of aquatic life. Canadian Environmental Quality Guidelines [Preprint].

Cánovas, C., Olías, M., Miguel Nieto, J., 2014. Metal(loid) Attenuation Processes in an Extremely Acidic River: the Rio Tinto (SW Spain). Springer. https://doi.org/10.1007/s11270-013-1795-7 [Preprint].

Cánovas, C.R., Olías, M., Sarmiento, A.M., Nieto, J.M., Galván, L., 2012. Pollutant transport processes in the Odiel River (SW Spain) during rain events. Water Resour. Res. 48 (6). https://doi.org/10.1029/2011WR011041.

Cánovas, C.R., Riera, J., Carrero, S., Olías, M., 2018. Dissolved and particulate metal fluxes in an AMD-affected stream under different hydrological conditions: the Odiel river (SW Spain). Catena 165, 414–424. https://doi.org/10.1016/j.catena.2018.02.020.

Coulthard, T.J., Macklin, M.G., 2003. Modeling long-term contamination in river systems from historical metal mining. Geology 31 (5), 451. https://doi.org/10.1130/0091-7613(2003)031<0451:MLCIRS>2.0.CO, 2.

Crane, R.A., Sapsford, D.J., 2018. Selective formation of copper nanoparticles from acid mine drainage using nanoscale zerovalent iron particles. J. Hazard Mater. 347, 252–265. https://doi.org/10.1016/j.jhazmat.2017.12.014.

Dold, B., 2014. Evolution of acid mine drainage formation in sulphidic mine tailings. Minerals 4 (3), 621–641. https://doi.org/10.3390/min4030621.

Dzombak, D.A., Francois, M.M., 1990. Surface Complexation Modeling: Hydrous Ferric Oxide. John Wiley and Sons.

Embrey, P.G., Symes, R.F., 1987. *Minerals of Cornwall and Devon., Minerals of Cornwall and Devon* . Tuscon, Arizona. British Museum Natural History and the Mineralogical Record Inc., London. https://encore.exeter.ac.uk/iii/encore/plus/C_SMinerals.of.Cornwall.and.Devonembrey.andsymes_Orightresult_U_X0?lang=eng&link=https%3A%2F%2Fuoelibrary.idm.oclc.org%2Flogin%3Furl%3Dhttp%3A%2F%2Fsearch.ebscohost.com%2Flogin.aspx%3Fdirect%3Dtrue%26site%3Deds-live%26db%3Dcat07716a%26AN%3Dpclc.99697763405136&suite=cobalt. (Accessed 19 November 2020).

Environment Agency, 2008. Abandoned Mines and the Water Environment. Environment Agency Science. *Report SC030136/SR41* [Preprint].

Environment Agency, 2020a. Lower river carnon, catchment data explorer. https://environment.data.gov.uk/catchment-planning/WaterBody/GB108048001231. (Accessed 15 March 2021).

Environment Agency, 2020b. Upper carnon river, catchment data explorer. https://environment.data.gov.uk/catchment-planning/WaterBody/GB108048001160. (Accessed 15 March 2021).

Equeenuddin, S.M., Tripathy, S., Sahoo, P.K., Panigrahi, M.K., 2013. Metal behavior in sediment associated with acid mine drainage stream: role of pH. J. Geochem. Explor. 124, 230–237. https://doi.org/10.1016/j.gexplo.2012.10.010.

Espinosa, E., Armienta, M.A., Cruz, O., Aguayo, A., Ceniceros, N., 2009. Geochemical distribution of arsenic, cadmium, lead and zinc in river sediments affected by tailings in Zimapán, a historical polymetalic mining zone of México. Environ. Geol. 58 (7), 1467. https://doi.org/10.1007/s00254-008-1649-6.

Foulds, S.A., Brewer, P., Macklin, M., 2012. Causes and Consequences of a Large Summer Storm and Flood in West Wales, 8th-9th June 2012. Fluvio.

Gerdelidani, A.F., Towfighi, H., Shahbazi, K., Lamb, D.T., Choppala, G., Abbasi, S., Bari, A.S.M.F., Naidu, R., Rahman, M.M., 2021. Arsenic geochemistry and mineralogy as a function of particle-size in naturally arsenic-enriched soils. J. Hazard Mater. 403, 123931. https://doi.org/10.1016/j.jhazmat.2020.123931.

GOV UK, 2025. Long term flood risk. https://www.gov.uk/check-long-term-flood-risk.

Hierro, A., Olías, M., Ketterer, M.E., Vaca, F., Borrego, J., Cánovas, C.R., Bolivar, J.P., 2014. Geochemical behavior of metals and metalloids in an estuary affected by acid mine drainage (AMD). Environ. Sci. Pollut. Control Ser. 21 (4), 2611–2627. https://doi.org/10.1007/s11356-013-2189-5.

Hudson-Edwards, K., Jamieson, H.E., Lottermoser, B.G., 2011. Mine wastes: past, present, future. Elements 7 (6), 375–380. https://vle.exeter.ac.uk/pluginfile.php/2418807/mod_resource/content/1/Hudson-Edwardsetal2011Elements.pdf. (Accessed 6 January 2021).

Hudson-Edwards, K., Macklin, M., Brewer, P., Dennis, I., 2008. Assessment of metal mining contaminated river sediments in England and Wales. Science Report: SC030136/SR4. Environment Agency [Preprint]. https://www.gov.uk/government/publications/assessment-of-metal-mining-contaminated-river-sediments-in-england-and-wales. (Accessed 30 May 2023).

Hudson-Edwards, K.A., Macklin, M.G., Jamieson, H.E., Brewer, P.A., Coulthard, T.J., Howard, A.J., Turner, J.N., 2003. The impact of tailings dam spills and clean-up operations on sediment and water quality in river systems: the Ríos Agrio–Guadiamar, Aznalcóllar, Spain Mark Macklin and P. Brewer - Academia.edu. Appl. Geochem. 221–239. https://www.academia.edu/34290966/The_impact_of_tailings_dam_spills_and_clean_up_operations_on_sediment_and_water_quality_in_river_systems_the_Rı_os_Agrio_Guadiamar_Aznalcóllar_Spain. (Accessed 22 March 2022).

Hudson-Edwards, K.A., Macklin, M.G., Miller, J.R., Lechler, P.J., 2001. Sources, distribution and storage of heavy metals in the Río Pilcomayo, Bolivia. J. Geochem. Explor. 72 (3), 229–250. https://doi.org/10.1016/S0375-6742(01)00164-9.

Hudson-Edwards, K.A., Schell, C., Macklin, M.G., 1999. Mineralogy and geochemistry of alluvium contaminated by metal mining in the Rio Tinto area, southwest Spain. Appl. Geochem. 14 (8), 1015–1030. https://doi.org/10.1016/S0883-2927(99)00008-6.

Hunt, L.E., Howard, A.G., 1994. Arsenic speciation and distribution in the Carnon estuary following the acute discharge of contaminated water from a disused mine. Mar. Pollut. Bull. 28 (1), 33–38. https://doi.org/10.1016/0025-326X(94)90183-X.

Izaditame, F., Siebecker, M.G., Sparks, D.L., 2022. Sea-level-rise-induced flooding drives arsenic release from coastal sediments. J. Hazard Mater. 423, 127161. https://doi.org/10.1016/j.jhazmat.2021.127161.

Jarvis, A.P., Davis, J.E., Orme, P.H., Potter, H.A., Gandy, C.J., 2019. Predicting the benefits of mine water treatment under varying hydrological conditions using a synoptic mass balance approach. Environ. Sci. Technol. 53 (2), 702–709. https://doi.org/10.1021/ACS.EST.8B06047/ASSET/IMAGES/LARGE/ES-2018-06047C_0005.JPEG.

Jennings, E., Onnis, P., Crane, R., Comber, S.D.W., Byrne, P., Riley, A.L., Mayes, W.M., Jarvis, A.P., Hudson-Edwards, K.A., 2025. Spatial and temporal (annual and decadal) trends of metal(loid) concentrations and loads in an acid mine drainage-affected river. Sci. Total Environ. 964, 178496. https://doi.org/10.1016/j.scitotenv.2025.178496.

Johnson, D.B., Hallberg, K.B., 2005. Acid mine drainage remediation options: a review. Sci. Total Environ. 338 (1–2), 3–14. https://doi.org/10.1016/J.SCITOTENV.2004.09.002.

Johnson, C.A., Thornton, I., 1987. Hydrological and chemical factors controlling the concentrations of Fe, Cu, Zn and as in a river system contaminated by acid mine drainage. Water Res. 21 (3), 359–365. https://doi.org/10.1016/0043-1354(87)90216-8.

Kim, C.S., Wilson, K.M., Rytuba, J.J., 2011. Particle-size dependence on metal(loid) distributions in mine wastes: implications for water contamination and human exposure. Appl. Geochem. 26 (4), 484–495. https://doi.org/10.1016/J.APGEOCHEM.2011.01.007.

Lottermoser, B.G., 2015. Predicting Acid Mine Drainage: past, Present, Future. *Mining Report* [Preprint].

Lynch, S.F.L., Batty, L.C., Byrne, P., 2014. Environmental risk of metal mining contaminated river bank sediment at redox-transitional zones. Minerals 2014 4, 52–73. https://doi.org/10.3390/MIN4010052, 4(1), pp. 52–73.

Macklin, M.G., Brewer, P.A., Hudson-Edwards, K.A., Bird, G., Coulthard, T.J., Dennis, I. A., Lechler, P.J., Miller, J.R., Turner, J.N., 2006. A geomorphological approach to the management of rivers contaminated by metal mining. Geomorphology 79 (3–4), 423–447. https://doi.org/10.1016/J.GEOMORPH.2006.06.024.

Macklin, M.G., Hudson-Edwards, K.A., Dawson, E.J., 1997. The significance of pollution from historic metal mining in the Pennine orefields on river sediment contaminant fluxes to the North Sea. Sci. Total Environ. 194–195, 391–397. https://doi.org/10.1016/S0048-9697(96)05378-8.

Macklin, M.G., Thomas, C.J., Mudbhatkal, A., Brewer, P.A., Hudson-Edwards, K.A., Lewin, J., Scussolini, P., Eilander, D., Lechner, A., Owen, J., Bird, G., Kemp, D., Mangalaa, K.R., 2023. Impacts of metal mining on river systems: a global assessment. Science 381 (6664), 1345–1350. https://doi.org/10.1126/science.adg6704.

Mayes, W.M., Potter, H.A.B., Jarvis, A.P., 2010. Inventory of aquatic contaminant flux arising from historical metal mining in England and Wales. Sci. Total Environ. 408 (17), 3576–3583. https://doi.org/10.1016/j.scitotenv.2010.04.021.

Millward, G.E., 1995. Processes affecting trace element speciation in estuaries. A review. Analyst 120 (3), 609. https://doi.org/10.1039/an9952000609.

Moreno-González, R., Macías, F., Olías, M., Ruiz Cánovas, C., 2022. Temporal evolution of acid mine drainage (AMD) leachates from the abandoned tharsis mine (Iberian Pyrite belt, Spain). Environ. Pollut. 295, 118697. https://doi.org/10.1016/J.ENVPOL.2021.118697.

Navarro Torres, V., Aduvire, O., Singh, R., 2012. Assessment of natural attenuation of acid mine drainage pollutants in El Bierzo and Odiel basins: a case study. Journal of Mining and Environment 2 (2), 78–85. https://doi.org/10.22044/JME.2012.70.

Neal, C., Whitehead, P.G., Jeffery, H., Neal, M., 2005. The water quality of the river carnon, west cornwall, November 1992 to March 1994: the impacts of wheal Jane discharges. Sci. Total Environ. 338 (1–2 SPEC. ISS.), 23–39. https://doi.org/10.1016/j.scitotenv.2004.09.003.

Nordstrom, D.K., Blowes, D.W., Ptacek, C.J., 2015. Hydrogeochemistry and microbiology of mine drainage: an update. Appl. Geochem. 57, 3–16. https://doi.org/10.1016/J.APGEOCHEM.2015.02.008.

Onnis, P., Byrne, P., Hudson-Edwards, K.A., Frau, I., Stott, T., Williams, T., Edwards, P., Hunt, C.O., 2023a. Source apportionment of mine contamination across streamflows. Appl. Geochem. 151, 105623. https://doi.org/10.1016/j.apgeochem.2023.105623.

Onnis, P., Byrne, P., Hudson-Edwards, K.A., Stott, T., Hunt, C.O., 2023b. Fluvial morphology as a driver of lead and zinc geochemical dispersion at a catchment scale. Minerals 13 (6), 790. https://doi.org/10.3390/min13060790.

Ortiz-Castillo, J., Mirazimi, M., Mohammadi, M., Dy, E., Liu, W., 2021. The role of microorganisms in the formation, dissolution, and transformation of secondary minerals in mine rock and drainage: a review. Minerals 11 (12), 1349. https://doi.org/10.3390/min11121349.

Papaslioti, E.M., Giampouras, M., Sánchez-López, L., Basallote, M.D., Freydier, R., Cánovas, C.R., Pérez-López, R., 2024. Temporal dynamics of contaminants in an estuarine system affected by acid mine drainage discharges. Sci. Total Environ. 947, 174683. https://doi.org/10.1016/J.SCITOTENV.2024.174683.

Pirrie, D., Power, M.R., Rollinson, G., Camm, G.S., Hughes, S.H., Butcher, A.R., Hughes, P., 2003. The spatial distribution and source of arsenic, copper, tin and zinc within the surface sediments of the Fal Estuary, Cornwall, UK. Sedimentology 50 (3), 579–595. https://doi.org/10.1046/j.1365-3091.2003.00566.x.

Pirrie, D., Power, M.R., Rollinson, G., Hughes, S.H., Camm, S.G., Watkins, D.C., 2002. Mapping and visualisation of historical mining contamination in the Fal Estuary, Cornwall, Camborne school of Mines. https://projects.exeter.ac.uk/geomincentre/estuary/home.htm. (Accessed 11 March 2021).

Rainbow, P.S., 2020. Mining-contaminated estuaries of Cornwall - Field research laboratories for trace metal ecotoxicology. Journal of the Marine Biological Association of the United Kingdom. Cambridge University Press, pp. 195–210. https://doi.org/10.1017/S002531541900122X.

Rezaie, B., Anderson, A., 2020. Sustainable resolutions for environmental threat of the acid mine drainage. Sci. Total Environ. 717, 137211. https://doi.org/10.1016/J.SCITOTENV.2020.137211.

Rodriguez-Freire, L., Avasarala, S., Ali, A.-M.S., Agnew, D., Hoover, J.H., Artyushkova, K., Latta, D.E., Peterson, E.J., Lewis, J., Crossey, L.J., Brearley, A.J., Cerrato, J.M., 2016. Post gold king mine spill investigation of metal stability in water and sediments of the animas river watershed. Environ. Sci. Technol. 50 (21), 11539–11548. https://doi.org/10.1021/acs.est.6b03092.

Scrivener, R.C., Shepherd, T.J., 1998. Mineralisation. In: Selwood, E.M. (Ed.), *The Geology of Cornwall*. Exeter. University of Exeter press, pp. 136–157.

Simate, G.S., Ndlovu, S., 2014. Acid mine drainage: challenges and opportunities. J. Environ. Chem. Eng. 2 (3), 1785–1803. https://doi.org/10.1016/j.jece.2014.07.021.

Sánchez Espańa, J., Pamo, E.L., Pastor, E.S., AndrÉs, J.R., RubÍ, J.A.M., 2006. The impact of acid mine drainage on the water quality of the Odiel river (Huelva, Spain): evolution of precipitate mineralogy and aqueous geochemistry along the concepción-tintillo segment. Water Air Soil Pollut. 173 (1–4), 121–149. https://doi.org/10.1007/s11270-005-9033-6.

Song, Y., Wilson, M., Moon, H.-S., Bacon, J., Bain, D., 1999. Chemical and mineralogical forms of lead, zinc and cadmium in particle size fractions of some wastes, sediments and soils in Korea. Appl. Geochem. 14 (5), 621–633. https://doi.org/10.1016/S0883-2927(98)00093-6.

Tremblay, G., Hogan, C., 2016. Mine environment neutral drainage (MEND) manual 5.4.2d: prevention and control. Canada Centre for Mineral and Energy Technology, Natural Resources (5.4. 2d), 1–23. Canada, Ottawa.

Turner, J.N., Brewer, P.A., Macklin, M.G., 2008. Fluvial-controlled metal and as mobilisation, dispersal and storage in the Río Guadiamar, SW Spain and its implications for long-term contaminant fluxes to the Doñana wetlands. Sci. Total Environ. 394 (1), 144–161. https://doi.org/10.1016/J.SCITOTENV.2007.12.021.

Warr, L.N., 2021. IMA–CNMNC approved mineral symbols. Mineral. Mag. 85 (3), 291–320. https://doi.org/10.1180/mgm.2021.43.

Wei, L., Liu, Y., Cai, D., Li, F., Luo, D., Li, C., Xu, G., Xiao, T., Wu, Q., He, H., Routh, J., 2022. River morphology redistributes potentially toxic elements in acid mine drainage-impacted river sediments: evidence, causes, and implications. Catena 214, 106183. https://doi.org/10.1016/j.catena.2022.106183.

Wolkersdorfer, C., 2008. Water Management at Abandoned Flooded Underground Mines: Fundamentals, Tracer Tests, Modelling, Water Treatment. Springer Science & Business Media. https://books.google.co.uk/books?hl=en&lr=&id=tHuu7QtUurwC&oi=fnd&pg=PR9&dq=Water+Management+at+Abandoned+Flooded+Underground+Mines+—+Fundamentals,+Tracer+Tests,+Modelling,+Water+Treatment&ots=_2P_KwWF9T&sig=RvT0IQhcZCJCFq7kkCZvdjhyDpo#v=onepage&q=Water

.Management.at.Abandoned.Flooded.Underground.Mines—Fundamentals%2C.Tracer.Tests%2C.Modelling%2C.Water.Treatment&f=false. (Accessed 19 May 2023).
Wołowiec, M., Komorowska-Kaufman, M., Pruss, A., Rzepa, G., Bajda, T., 2019. Removal of heavy metals and metalloids from water using drinking water treatment residuals as adsorbents: a review. Minerals 9 (8), 487. https://doi.org/10.3390/min9080487.
Ye, Z., Zhou, J., Liao, P., Finfrock, Y.Z., Liu, Y., Shu, C., Liu, P., 2022. Metal (Fe, Cu, and As) transformation and association within secondary minerals in neutralized acid mine drainage characterized using X-ray absorption spectroscopy. Appl. Geochem. 139, 105242. https://doi.org/10.1016/j.apgeochem.2022.105242.
Zhang, H., Yu, J., Zhou, S., 2014. Spatial distribution of As, Cr, Pb, Cd, Cu, and Zn in the water and sediment of a river impacted by gold mining. Mine Water Environ. 33 (3), 206–216. https://doi.org/10.1007/s10230-013-0254-4.